Non-ideal MHD ballooning modes in three-dimensional configurations

T. Rafiq, C. C. Hegna and J. D. Callen

University of Wisconsin, Madison,Wisconsin 53706-1609

A linear stability theory of non-ideal MHD ballooning modes is investigated using a two fluid model for arbitrary three-dimensional electron-ion plasmas. Resistive-inertia ballooning mode (RIBM) eigenvalues and eigenfunctions are calculated for a variety of equilibria including axisymmetric shifted circular geometry ($s-\alpha$ model) and configurations of interest to the Helically Symmetric Stellarator (HSX). For parameters of interest to HSX, characteristic growth rates exceed the electron collision frequency. In this regime, electron inertia effects dominate plasma resistivity and produce an instability whose growth rate scales with the electromagnetic skin depth. Attempts to generalize previous analytic calculations [1] of RBM stability using a two scale analysis on $s-\alpha$ equilibria to more general 3-D equilibria will be addressed.

Keywords: Drift, Resistive-inertia, Ballooning, Stellarator, HSX

Unstable resistive ballooning modes (RBM) may play an important role in producing edge plasma fluctuations and anomalous transport in tokamaks and stellarators. In this work, the stability criterion for non-ideal MHD ballooning modes is derived for arbitrary three-dimensionally ideal MHD stable electron-ion plasmas. In the presence of non-ideal effects, ballooning instabilities can be produced at plasma β levels below the critical β for ideal ballooning stability. Electron inertia, diamagnetic effects, parallel ion dynamics, transverse particle diffusion and perpendicular viscous stress terms are included in the calculations. Temperature perturbations and equilibrium temperature gradients are ignored for simplicity. For parameters of interest to the Helically Symmetric Experiment (HSX), characteristic growth rates exceed the electron collision frequency. In this regime, electron inertia effects can dominate plasma resistivity and produce an instability whose growth rate scales with the electromagnetic skin depth.

In this work, a unified theory of RBM and inertial ballooning modes is developed where both the effects of ideal MHD free energy (as measured by the asymptotic matching parameter Δ') and geodesic curvature drives in the non-ideal layer are included in the dispersion relation. This theory may explain the $k_y \leq 1/cm$ fluctuations and the anomalous plasma transport observed in HSX near $r/a = 0.7$ where $T_e = 100eV$. Resistive-inertia ballooning mode (RIBM) eigenvalues and eigenfunctions are numerically calculated for a variety of equilibria including axisymmetric shifted circular geometry ($s-\alpha$ model) and configurations of interest to the HSX.

The organization of this paper is as follows. In section I, linearized ballooning equations are derived from Ohm's law, vorticity, continuity and parallel momentum equations. In section II, RIMHD modes are numerically calculated for $\hat{s}-\alpha$ equilibria and for quasihelically symmetric stellarator (QHS) equilibria in the electrostatic limit. The results for QHS are compared and contrasted with a magnetic configuration that spoils the helical symmetry by adding mirror terms to the magnetic spectrum. In section III, the shear Alfvén and drift acoustic equations in general 3-D geometry are presented in Hamada coordinates using a multiple length scale analysis. Section IV is devoted to study of these equations using a multiple length scale expansion technique and derivation of the dispersion relation. In section V, we summarize the results.

author's e-mail: rafiq@engr.wisc.edu

I. Drift ballooning equations

The reduced Braginskii fluid equations for a four-field model of drift resistive ballooning modes are used. The equations for generalized Ohm's law, vorticity, electron continuity and total parallel momentum can take the following linearized form in an $\omega \sim \omega_s \sim \omega_{*j} \sim \omega_\eta$ ordering

$$\left(\omega - \omega_{*en} + \omega H + ic^2 k_\perp^2 \eta_\parallel/4\pi\right)\widehat{\Psi} = c_s k_\parallel \left(\widehat{\Phi} - \widehat{n}\right), \tag{1}$$

$$\omega k_\perp^2 \rho_i^2 \left(\widehat{n} + \tau\widehat{\Phi}\right) = \omega_\kappa \widehat{n} - i\mu_\perp k_\perp^4 \rho_i^2 \left(\widehat{n} + \tau\widehat{\Phi}\right) + \frac{\tau v_A^2}{c_s} k_\parallel \left(k_\perp^2 \rho_i^2 \widehat{\Psi}\right), \tag{2}$$

$$\omega\widehat{n} - \omega_{*en}\widehat{\Phi} = \omega_{\kappa e}\left(\widehat{\Phi} - \widehat{n}\right) + c_s k_\parallel \widehat{\mathbf{v}}_\parallel + \frac{i\eta_\perp c^2 k_\perp^2}{4\pi}\frac{c_s^2}{v_A^2}\widehat{n} - \frac{\tau v_A^2}{c_s} k_\parallel \left(k_\perp^2 \rho_i^2 \widehat{\Psi}\right), \tag{3}$$

$$(\omega + \omega_{\kappa i})\widehat{\mathbf{v}}_\parallel + \omega_{*en}\widehat{\Psi} = c_s k_\parallel \widehat{n} - 4i\mu_\perp k_\perp^2 \widehat{v}_\parallel, \tag{4}$$

where $H = k_\perp^2 \delta_e^2$, $\delta_e^2 = c^2/\omega_{pe}^2$, is the electromagnetic skin depth, $\omega_{pe}^2 = 4\pi n e^2/m_e$, is the electron plasma frequency, $\mu_\perp = 0.3\nu_i \rho_i^2$, is the classical perpendicular viscosity, $\rho_i = v_{ti}/\omega_{ci}$, is the ion Larmor radius, $v_{ti} = \sqrt{T_i/m_i}$, is the ion thermal velocity, $\omega_{ci} = eB/m_i c$, is the ion cyclotron frequency, $\tau = T_e/T_i$, is the electron to ion temperature ratio, $v_A^2 = B^2/4\pi n m_i$, is the Alfvén speed, $\eta_\parallel$ and $\eta_\perp$ are the longitudinal and transverse Spitzer resistivities. $\widehat{\Psi} = e c_s \widetilde{A}_\parallel / c T_e$, $\widehat{\Phi} = e\widetilde{\phi}/T_e$, $\widehat{v}_\parallel = \widetilde{v}_\parallel / c_s$,

$\widehat{n} = \widetilde{n}/n$, are the dimensionless perturbed parallel component of vector potential, electrostatic potential, parallel ion flow and density, respectively. Also $\omega_\kappa = \omega_{\kappa i} + \omega_{\kappa e}$, where $\omega_{\kappa j} = \left(2cT_j/eB\right)\mathbf{k}\cdot\widehat{e}_\parallel \times \kappa$, $c_s = (T_e + T_i/m_i)^{1/2}$, $\omega_{*en} = -\left(cT_e/eB\right)\mathbf{k}\cdot\widehat{e}_\parallel \times \nabla \ln n$, are the curvature drift frequency, sound speed and the diamagnetic drift frequency.

The resistive-inertia MHD incompressible ballooning equation for high frequency ($|\omega| \gg \omega_{*e}, \omega_{\kappa e}$) long wavelength ($k_\theta^2\rho_i^2 \ll 1$)limit can be written as follows:

$$\omega_A^2 \frac{d}{d\theta}\left(\frac{\widehat{k}_\perp^2}{\omega + (\omega c^2 k_\theta^2/\omega_{pe}^2 + i\omega_\eta)\widehat{k}_\perp^2}\frac{d\widehat{\Phi}}{d\theta}\right) + (\omega \widehat{k}_\perp^2 + \frac{\tau' \omega_{\kappa e}\omega_{*e}}{\omega k_\theta^2 \rho_s^2})\widehat{\Phi} = 0, \quad (5)$$

where $\omega_A = v_A/qR$, is the Alfvén frequency, q is the safety factor and R is the major radius, $\epsilon_n = L_n/R$, with $L_n = (d_r \ln n)^{-1}$, is the density gradient scale length, $k_\parallel = -i(1/qR)d/d\theta$, $k_\perp = \left(n_\phi q/r\right)\widehat{k}_\perp(\theta)$. $\omega_\eta = \left(c^2\eta_\parallel/4\pi\right)\left(n_\phi q/r\right)^2$, is the resistive frequency and $\tau' = 1 + 1/\tau$. Note that in Eq. (5) the electron inertia term, $\omega c^2 k_\theta^2/\omega_{pe}^2$ is present. The incompressible ideal MHD (IMHD) ballooning equation can be retained by neglecting electron inertia and resistivity.

II. Numerical results

Equation (5) is solved numerically using a standard root finding algorithm for axisymmetric shifted-circle equilibrium (in Figures 1 and 2) and for three dimensional equilibria of relevance to HSX (Figure 3). For all cases, the parameters used are relevant to HSX edge plasmas, as indicated in the caption of Fig.1.

Figure 1 shows the normalized growth rate (γ/ω_A) as a function of the normalized pressure gradient (the ballooning parameter α). In this scan, tokamak-like global magnetic shear $\hat{s} = 0.1$ is chosen to show the ideal MHD unstable region. HSX has reverse shear and ideal MHD instabilities for which the mode amplitude does not vary along the field line (i.e., $k_\parallel$=0) are stable for the parameters studied. The electron inertia and resistivity induce an instability in the ideal MHD stable regimes. The modes are purely growing $\omega_r = 0$. The electron inertia modes ($\eta = 0$) are found to be more important than the resistive modes due to their existence in the first ideal stability region for HSX relevant parameters. Note that these modes persist in the ideal MHD second stable regime. Both the electron inertia and resistive instabilities are characterized by broad eigenfunctions in the ballooning space as shown in Fig. 2. Moreover, the qualitative nature of the eigenfunctions is insensitive to whether electron inertia is present.

Equation (5) is solved numerically in the electrostatic limit using three dimensional equilibria for a quasi-helically symmetric (QHS) stellarator and a configuration whose symmetry is spoiled (Mirror) by the presence of magnetic mirror contributions to the magnetic spectrum.

Figure 3 is a plot of the growth rate γ, normalized to the R/c_s as a function of $(k_\perp\rho)^2$. We perform this calculation for the field line that intersects the location $\theta_0 = 0$,

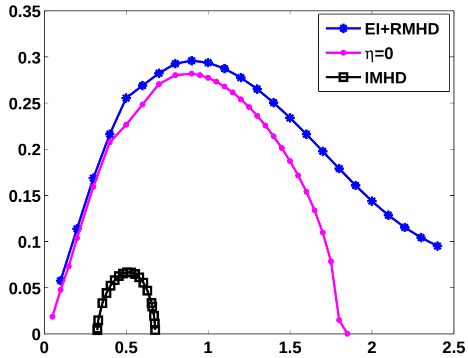

Fig. 1 The normalized growth rate (γ/ω_A) as a function of α for $\hat{s} = 0.1$, $k_\theta\rho = 0.3$, $\hat{\nu} = 0.023$, and $\beta = 0.0002$.

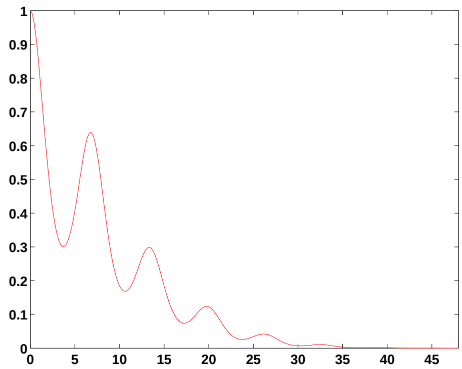

Fig. 2 Eigenfunction of RIBM as a function of θ for $\alpha = 0.3$. The other parameters are the same as used in figure 1.

$\zeta_0 = 0$ on the normalized magnetic surface $s = 0.8980$. This point is thought to be the most unstable choice since the local shear is small, the local value of the geodesic curvature is zero and the destabilizing influence of the normal curvature is strongest. The highly resistive ($\delta = 0$, $\nu \neq 0$) growth rate in QHS is compared with the growth rate in the Mirror case. In both configurations the magnitude of the linear growth rates are found to be comparable, crudely indicating the same level of anomalous flux. The common stability properties are due to a similar structure of the curvature and the local magnetic shear.

III. Shear-Alfvén and Drift acoustic equation in 3-D geometry

The general solution of Eqs. (1)-(4) can be written as a coupled system of a two second order differential equations, the shear-Alfvén equation and the drift-acoustic equation:

$$\frac{d}{dy}\left[\frac{(\omega - \omega_{ne})K^2 dU/dy}{B^2(\omega - \omega_{ne} + (\omega\delta_e^2 + i\eta^*)a^2K^2)}\right] + \frac{8\pi p^{\cdot}\left(\kappa_\nu + q^{\cdot}y\kappa_\varphi\right)}{\chi^{\cdot 4}}$$
$$\times(U+V) = -\frac{K^2}{\chi^{\cdot 2}v_A^2}\left(\omega + i\mu_\perp a^2K^2\right)\left[(\omega - \omega_{ni})U - (1+\tau)\omega_{ni}V\right], \quad (6)$$

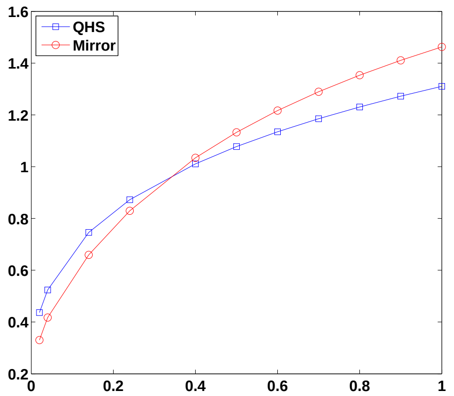

Fig. 3 Normalized growth rate $(R\gamma/C_s)$ of the resistive-inertia ballooning modes in the electrostatic limit as a function of $(k_\perp\rho)^2$ for QHS and Mirror cases for $s = 0.8980$, $\tau = 1$, $Rv/2c_s = 0.42$, $\epsilon_n = 0.07$ and $\theta_0 = 0$, $\zeta_0 = 0$ field line.

and

$$\frac{d}{dy}\left(\frac{\chi'^2}{B^2}\frac{dV}{dy}\right)+\frac{(\omega-\omega_{ne})\left(\omega+4i\mu_\perp a^2K^2\right)}{c_s^2}V=$$
$$\left[-\frac{\left(\omega+4i\mu_\perp a^2K^2\right)}{c_s^2}\left(2L_{nv}\left(\kappa_v+q'y\kappa_\varphi\right)+\frac{\tau\omega a^2K^2\rho_i^2}{\omega_{ne}}\right)\right.$$
$$\left.+\frac{\left(\omega\delta_e^2+i\eta^*\right)\left(\omega+i\mu_\perp a^2K^2\right)}{\omega-\omega_{ne}}\frac{a^2K^2}{v_A^2}\right]\left[(\omega-\omega_{ni})\,U-(1+\tau)\,\omega_{ni}V\right]$$
$$+\left[\left(\frac{\omega\delta_e^2+i\eta^*}{\omega-\omega_{ne}}\right)\frac{8\pi a^2p'\left(\kappa_v+q'y\kappa_\varphi\right)}{\chi'^2}-\frac{\eta_\perp}{\eta_\parallel}\frac{i\eta^*\left(\omega+4i\mu_\perp a^2K^2\right)a^2K^2}{v_A^2}\right]$$
$$\times(U+V)+\frac{\chi'^2}{B^2}\frac{d}{dy}\ln\left(\omega+4i\mu_\perp a^2k_\perp^2\right)$$
$$\times\left[\frac{\left(\omega\delta_e^2+i\eta^*\right)a^2K^2}{\omega-\omega_{*e}+\left(\omega\delta_e^2+i\eta^*\right)a^2K^2}\frac{dU}{dy}+\frac{dV}{dy}\right], \qquad (7)$$

where $K^2 = |\nabla\varphi|^2 - 2q'y\nabla\varphi\cdot\nabla v + q'^2y^2|\nabla v|^2$, $a = \partial S/\partial\varphi$, is the "mode number" that describes the component of the **k** vector that is perpendicular to the magnetic field and lies within the magnetic surface, $\kappa_v = \kappa\cdot\nabla\theta\times\nabla\varphi$, $\kappa_\varphi = \kappa\cdot\nabla v\times\nabla\theta = (-\chi'/2p')\mathbf{B}\cdot\nabla\sigma$, is the geodesic curvature and $\sigma = \mathbf{j}\cdot\mathbf{B}/B^2$. The coordinate y is defined as labeling points along the magnetic field and as such $\mathbf{B}\cdot\nabla = \chi'(d/dy)$. Dot over quantities indicate derivatives with respect to the volume.

IV. Analysis of Resistive Ballooning Mode equations

We can make analytic progress to understand the structure of non-ideal MHD ballooning modes by using a multiple scale analysis. Our calculation generalizes the work of Hastie et al [1] to three-dimensional equilibria. A small parameter ϵ can be defined that accounts for the disparate timescales associated with current diffusion and the Alfvén time.

$$\epsilon = \left(\frac{\omega_\eta}{\omega_A}\right)^{1/3} \ll 1, \qquad (8)$$

In the following, somewhat general ordering is used

$$\omega \sim \omega_s \sim \omega_{nj} \sim \epsilon\omega_A \qquad (9)$$

and viscosity is comparable to resistivity, $\omega_\mu = \epsilon^3\omega_A$. Equations (6,7) can be solved using a two variable expansion procedure. We take y and $z = \epsilon y$ as two different length scales and make the ansatz

$$U(y) = U_0(y,z) + \epsilon U_1(y,z) + \epsilon^2 U_2(y,z) + ... \qquad (10)$$

$$U_i(y+N,z) = U_i(y,z), \quad i = 0,1,2,... \qquad (11)$$

The function U is periodic in y with period N whereas the variable z accounts for the long envelope of the eigenfunction along the magnetic field line. For $|y| \sim 1$ an ideal MHD region can be identified where resistivity, electron inertia and viscosity can be neglected. The Shear Alfvén equations in the zeroth order in ϵ can be written as

$$\frac{d}{dy}\left[\frac{K^2}{B^2}\frac{dU_0}{dy}\right]+\frac{4\pi}{\chi'^4}\left(2p'\kappa_v - q'\chi'^2y\frac{d\sigma}{dy}\right)U_0 = 0. \qquad (12)$$

At large $|y|$, the solution of the Shear Alfvén equation yields the following asymptotic solution

$$U = a_1|y|^s + a_2|y|^{-1-s}, \quad |y|\to\infty, \qquad (13)$$

where

$$s = -\frac{1}{2}+\left[\frac{1}{4}+H^2-H-D_R\right]^{1/2}. \qquad (14)$$

The quantities H and D_R are dependent upon the equilibrium and are defined as [3]

$$H = \frac{A^2\langle B^2/\left|\widehat{\nabla v}\right|^2\rangle}{q'\chi'^2}\left[\frac{\langle\sigma B^2\rangle}{\langle B^2\rangle}-\frac{\langle\sigma B^2/\left|\widehat{\nabla v}\right|^2\rangle}{\langle B^2/\left|\widehat{\nabla v}\right|^2\rangle}\right], \qquad (15)$$

$$D_R = F + E + H^2, \qquad (16)$$

$$F = \frac{A^2\langle B^2/\left|\widehat{\nabla v}\right|^2\rangle}{q'^2\chi'^4}\left[\langle\frac{B^2\sigma^2}{\left|\widehat{\nabla v}\right|^2}\rangle-\frac{\langle\sigma B^2/\left|\widehat{\nabla v}\right|^2\rangle^2}{\langle B^2/\left|\widehat{\nabla v}\right|^2\rangle}+p'^2\langle\frac{1}{B^2}\rangle\right], (17)$$

$$E = \frac{A\langle B^2/\left|\widehat{\nabla v}\right|^2\rangle}{q'^2\chi'^4}\left[I'\Psi''-J'\chi''-q'\chi'^2\frac{\langle\sigma B^2\rangle}{\langle B^2\rangle}\right] \qquad (18)$$

For this analysis, thus, ideal stability is assumed; the Mercier stability criterion is satisfied

$$-D_I = \frac{1}{4}-(E+F+H) = \frac{1}{4}+H^2-H-D_R \geqq 0. (19)$$

In the outer region solution along field lines ($|y| \gtrsim \epsilon^{-1}$), resistivity, inertia and viscosity must be taken into account.

We solve Eq. (6) order by order. At second order a solubility condition for U_2 is derived that yields a differential equation for U_0 that depends upon integrals of U_1 and V_1

$$\left\langle \frac{\partial}{\partial z} \frac{q^{\cdot 2} z^2 \left|\widehat{\nabla} v\right|^2}{B^2 A_3} \frac{\partial U_1}{\partial y} \right\rangle = -\left\langle \frac{\partial}{\partial z} \frac{q^{\cdot 2} z^2 \left|\widehat{\nabla} v\right|^2}{B^2 A_3} \frac{\partial U_0}{\partial z} \right\rangle$$
$$-q^{\cdot 2} z^2 \left(\widehat{\omega} - \widehat{\omega}_{ni}\right) U_0 \left\langle \frac{\left|\widehat{\nabla} v\right|^2}{B^2} \left(\widehat{\omega} + i\widehat{\mu} q^{\cdot 2} z^2 \left|\widehat{\nabla} v\right|^2\right) \right\rangle$$
$$-\frac{A_1 q^{\cdot} z U_0}{\chi^{\cdot 2}} \left[\langle 2p^{\cdot} \kappa_v \rangle - q^{\cdot} z \chi^{\cdot 2} \left(\left\langle \frac{\partial \sigma}{\partial z} \right\rangle - \left\langle \left(\frac{\partial U_1}{\partial y} + \frac{\partial V_1}{\partial y} \right) \sigma \right\rangle \right) \right], \quad (20)$$

where $A_3 = 1 + q^{\cdot 2} z^2 \widehat{\omega}_{IR} \left|\widehat{\nabla} v\right|^2$. One special limit that can be pursued analytically is the electrostatic limit. In this case, $q^{\cdot 2} z^2 \widehat{\omega}_{IR} \left|\widehat{\nabla} v\right|^2 \gg 1$, and $V_1 = 0$,

$$\frac{d^2 U_0}{dz^2} + W_1 \left[\langle 2p^{\cdot} \kappa_v \rangle + q^{\cdot} \chi^{\cdot 2} \left(\langle \sigma \rangle - \frac{\langle \sigma B^2 \rangle}{\langle B^2 \rangle} \right) \right] U_0$$
$$= \quad -W_2 \left[\left\langle \sigma^2 B^2 \right\rangle - \frac{\left\langle \sigma B^2 \right\rangle^2}{\langle B^2 \rangle} - W_3 \left\langle \frac{\left|\widehat{\nabla} v\right|^2}{B^2} \right\rangle \right] z^2 U_0, \quad (21)$$

where

$$W_1 = \left(\frac{A}{\chi^{\cdot 4}}\right) \widehat{\omega}_{IR} \left\langle B^2 \right\rangle, \quad W_2 = \frac{q^{\cdot 2} \chi^{\cdot 4}}{\langle B^2 \rangle} W_1^2, \quad W_3 = \widehat{\omega} \left(\widehat{\omega} - \widehat{\omega}_{ni}\right) \frac{q^{\cdot 2} \left\langle B^2 \right\rangle}{W_2},$$

and

$$A = 4\pi \left(\overline{a}/q\right)^2 \quad \widehat{\omega}_{IR} = \frac{\widehat{\omega} \delta^2/\epsilon^2 + i}{\widehat{\omega} - \widehat{\omega}_{ne}}, \quad \widehat{\omega} = \frac{\omega}{\epsilon \omega_A}, \quad \widehat{\nabla} = \frac{\overline{a}}{q} \nabla.$$

The condition for existence of a solution is $2p^{\cdot} \langle \kappa_v \rangle + q^{\cdot 2} \chi^{\cdot 2} \left(\langle \sigma \rangle - \left\langle \sigma B^2 \right\rangle / \left\langle B^2 \right\rangle \right) > 0$. The solutions (21) give the following eigenvalue expression

$$\omega \left(\omega - \omega_{ne}\right) \left(\omega - \omega_{ni}\right) = -\frac{\omega_A^2 \left(\omega \delta^2 + i\omega_\eta\right)}{\left\langle \left|\widehat{\nabla} v\right|^2 / B^2 \right\rangle} \left(\frac{4\pi \left(\overline{a}/q\right)^2}{\chi^{\cdot 2}}\right)^2 \left[\left\langle \sigma^2 B^2 \right\rangle \right.$$
$$\left. -\frac{\left\langle \sigma B^2 \right\rangle^2}{\langle B^2 \rangle} + \frac{\left\langle B^2 \right\rangle}{\left(q^{\cdot 2} \chi^{\cdot 4} (2n+1)^2\right)} \times \left\{ \langle 2p^{\cdot} \kappa_v \rangle + q^{\cdot} \chi^{\cdot 2} \left(\langle \sigma \rangle - \frac{\langle \sigma B^2 \rangle}{\langle B^2 \rangle} \right) \right\}^2 \right]. \quad (22)$$

Solutions to the the above equation lead to an infinite sequence of modes with growth rate scaling as for the resistive ballooning mode, $\gamma \sim \omega_\eta^{1/3}$ or for the electron inertia ballooning mode $\gamma \sim \delta$.

In the limit $\omega \gg \omega_s$, $V_0 = V_1 = 0$, sound wave propagation is neglected and the visco-resistive-inertia ballooning mode equation can be found

$$\frac{\partial}{\partial X} \frac{X^2}{1+X^2} \frac{\partial U_0}{\partial X} + \frac{H(1-H)}{\left(1+X^2\right)^2} U_0 - \frac{H(1+H) X^2}{\left(1+X^2\right)^2} U_0$$
$$+D_R U_0 - Q_1 U_0 X^2 - Q_2 U_0 X^4 = 0, \quad (23)$$

In the limit of zero viscosity ($\omega_\mu = 0$), $Q_2 = 0$ in Eq. (23), and the drift resistive ballooning equation is recovered. This equation has the same form as the resistive MHD case covered in Ref. [2] except for the diamagnetic corrections evident in the coefficient Q_1 (defined in Eq.(25) below). A valid solution can be constructed in the ideal and resistive region by matching the ideal solution for $|y| \longrightarrow \infty$ to the resistive solution for $|X| \longrightarrow 0$. We obtain the general dispersion relation, $\Delta = \Delta'$, where Δ' can be calculated by using the conventional definition as the ratio of coefficients of the large and small solutions of the asymptotic form of the ideal solution, which in this case defined as $\Delta' \equiv a_2/a_1$, and

$$\Delta \quad \equiv \quad \frac{4 y_0^{1+2s} Q^{(5-2s)/4}}{Q_1 - (1+s-H)^2} \frac{\Gamma[1/2+s]}{\Gamma[-1/2-s]}$$
$$\times \frac{\Gamma\left[(1/4)\left(Q_1^{1/2} + 3 - 2s - D_R/Q_1^{1/2}\right)\right]}{\Gamma\left[(1/4)\left(Q_1^{1/2} + 1 + 2s - D_R/Q_1^{1/2}\right)\right]}, \quad (24)$$

where

$$Q_1 = \frac{\omega \left(\omega - \omega_{ni}\right) \left(\omega - \omega_{ne}\right)}{Q_0}, \quad Q_0 = \frac{q^{\cdot 2} \left\langle B^2 \right\rangle \omega_A^2 \left(\omega \delta^2 + i\omega_\eta\right)}{A N_1 M}, \quad (25)$$

$$X^2 = \frac{Z^2}{y_0^2 Q_1}, \quad y_0^2 = \frac{\omega_A^2}{A M \omega \left(\omega - \omega_{ni}\right)},$$

$$M = \left\langle \frac{B^2}{\left|\widehat{\nabla} v\right|^2} \right\rangle \left[\left\langle \left|\widehat{\nabla} v\right|^2 / B^2 \right\rangle + \frac{1}{p^{\cdot 2}} \left\{ \left\langle \sigma^2 B^2 \right\rangle - \frac{\left\langle \sigma B^2 \right\rangle^2}{\langle B^2 \rangle} \right\} \right]$$

and Γ is the gamma function. For the special case when $D_R > 0$, we also reproduce the stability criterion derived in Ref. [2] with electron inertia and diamagnetic corrections:

$$\omega \left(\omega - \omega_{ne}\right) \left(\omega - \omega_{ni}\right) = -\frac{\omega_A^2 \left(\omega \delta^2 + i\omega_\eta\right)}{A N_1 M} q^{\cdot 2} \left\langle B^2 \right\rangle$$
$$\times \left[\left\{ \left(\frac{1}{2} + s + 2n \right)^2 + D_R \right\}^{1/2} - \left(\frac{1}{2} + s + 2n \right) \right]^2. \quad (26)$$

V. Summary

A unified theory of resistive and electron inertia ballooning modes (RIBM) has been developed. The RIBM is characterized by broad eigenfunctions in ballooning space. In the absence of drift effects, the modes are purely growing and persist in regimes where ideal MHD ballooning modes are stable. For parameters of interest to HSX, electron inertia effects are more important than plasma resistivity; electron inertia modes are the most unstable and have growth rates that scale with the electron skin depth, $\gamma \sim \delta$. The magnitude of the linear growth rates are not sensitive to the magnetic configuration in HSX plasmas. This would indicate a comparable level of anomalous transport in QHS and mirror configurations; this is consistent with observations in the HSX edge region.

Acknowledgments

This research was supported by the U.S. DoE under Grant Nos. DE-FG02-99E54546 and DE-FG02-86ER53218.

[1] R. H. Hastie, J. J. Ramos and F. Porcelli, Phys. Plasmas **10**, 4405 (2003).

[2] D. Correa-Restrepo, Z. Naturforsch. A **37,** 848 (1982).

[3] A. H. Glasser, J. M. Greene and J. L. Johnson, Phys. of Fluids **18**, 875 (1975).